has a strong effect on the predictions. The vaporization behavior of a hexane fuel droplet is not sensitive to the vaporization models. However, for less volatile fuels such as decane, the vaporization behavior shows some sensitivity to the models. The thin-skin model is not as accurate as the other two models which show excellent agreement with experimental data.

(2) The vaporization behavior of a multicomponent fuel droplet is better simulated by the infinite-diffusion model. However, the difference between the infinite-diffusion and diffusion-limit models is not very significant. The thin-skin model shows significant deviation from the experimental values.

(3) The variable property effects are important for an accurate prediction of droplet velocity and size. Not only the effect of temperature but also that of fuel vapor should be considered for calculating the thermophysical properties of the gas film surrounding the droplet. For low ambient temperatures, the accurate evaluation of the latent heat of fuel also has a noticeable effect on predictions.

To conclude, the present study illustrates that for relatively low ambient temperatures, both the infinite-diffusion and diffusion-limit methods can accurately predict the vaporization of pure as well as multicomponent fuel droplets. However, it is important to include the effects of variable thermophysical properties of the gas film outside the droplet as well as of the liquid-phase properties in a comprehensive manner. The present study also indicates the need for measuring the surface properties of a vaporizing multicomponent fuel droplet.

*Acknowledgement*—The financial support from the Air Force Office of Scientific Research is gratefully acknowledged.

## REFERENCES

1. G. A. E. Godsave, Studies of the combustion of drops in a fuel spray—the burning of single drops of fuel, *Fourth Symposium (International) on Combustion*, p. 818. Williams and Wilkins, Baltimore (1953).
2. C. K. Law, Recent advances in droplet vaporization and combustion, *Prog. Energy Combust. Sci.* **8**, 169–199 (1982).
3. S. K. Aggarwal, A. Tong and W. A. Sirignano, A comparison of vaporization models in spray calculations, *AIAA J.* **22**, 1448–1457 (1984).
4. W. A. Sirignano, Theory of multicomponent fuel droplet vaporization, *Arch. Thermodyn. Combust.* **9**, 231–247 (1978).
5. R. B. Landis and A. F. Mills, Effect of internal diffusional resistance on the evaporation of binary droplets, Fifth Int. Heat Transfer Conf., Tokyo, Japan, Paper B7-9 (1974).
6. C. K. Law and H. K. Law, A $d^2$-law for multicomponent droplet vaporization and combustion, *AIAA J.* **20**, 522–527 (1982).
7. A. Y. Tong and W. A. Sirignano, Multicomponent droplet vaporization in a high temperature gas, *Combust. Flame* **66**, 221–235 (1986).
8. G. Chen, Vaporization behavior of pure and multicomponent fuel droplets in a hot air stream, M.S. Thesis, The University of Illinois at Chicago (1989).
9. G. A. Agoston, H. Wise and W. A. Rosser, Dynamic facts affecting the combustion of liquid spheres, *Sixth Symposium (International) on Combustion*, pp. 708–717. Reinhold, New York (1957).
10. R. A. Ingebo, Drag coefficients for droplets and solid spheres in clouds accelerating in air streams, NACA Technical Note 3762 (1956).
11. C. K. Law and F. A. Williams, Kinetics and convection in the combustion of alkane droplets, *Combust. Flame* **29**, 393–405 (1972).
12. T. A. Jackson, G. L. Switzer and S. K. Aggarwal, Measurements of droplet size and velocities in a laminar flow (under preparation).

*Int. J. Heat Mass Transfer.* Vol. 34, No. 10, pp. 2673–2676, 1991
Printed in Great Britain

0017–9310/91 $3.00 + 0.00


# Calculation of scattering fractions for use in radiative flux models

R. KOENIGSDORFF, F. MILLER and R. ZIEGLER

Deutsche Forschungsanstalt für Luft- und Raumfahrt, Institut für Technische Thermodynamik, Pfaffenwaldring 38/40, 7000 Stuttgart 80, Germany

(*Received* 15 *August* 1990)

## INTRODUCTION

ONE OF the most widely used methods to solve the equation of radiation transfer in participating media is the two-flux model. Apparently first introduced in the field of astrophysics where it is credited to Schuster and Schwarzchild [1], it has since been applied to problems in combustion, radiation transfer through insulation, solar energy absorption, atmospheric physics, and spectroscopy (where it is called Kubelka–Munk theory). The initial two-flux approximation, useful only for diffuse one-dimensional radiation transfer, has been extended to two and three dimensions—four and six fluxes respectively—and also has been modified to allow for partially collimated incident radiation. In the case of scattering media, factors that determine how the scattered light is distributed in the various axial directions appear in the flux equations. This note discusses and compares various methods of determining these scattering fractions for the two- and six-flux models starting from the properties of the scattering particles comprising the medium. Results are presented for two sample media, one purely scattering and one that also absorbs, and approximate methods for evaluating the scattering fractions are shown to be valid in certain ranges of the particle size parameter.

## TWO-FLUX MODEL

The derivation of the two-flux equations has been rigorously laid out by Brewster [2] and others and will not be repeated in detail here. Briefly, however, the general equation of transfer for radiative intensity $i'$ in a general direction $S$ in a non-emitting participating medium [1]

$$\frac{\mathrm{d}i'_\lambda}{\mathrm{d}S} = -a_\lambda i'_\lambda(S) - \sigma_{s\lambda} i'_\lambda(S) + \frac{\sigma_{s\lambda}}{4\pi}\int_{4\pi} i'_\lambda(S,\omega_i)\Phi(\lambda,\omega,\omega_i)\,\mathrm{d}\omega_i \quad (1)$$

is simplified by assuming that the intensity is constant within each of two opposed solid angles (which are hemispheres in the two flux case) corresponding to two coordinate axis directions, say $x$ and $-x$. This allows the integral in equation (1) to be solved for each hemisphere and results in the two equations

## NOMENCLATURE

| | |
|---|---|
| $a$ | absorption coefficient |
| $b$ | backward scattering fraction (six-flux model) |
| $B$ | backward scattering fraction (two-flux model) |
| $f$ | forward scattering fraction (six-flux model) |
| $i'$ | radiation intensity |
| $I$ | radiative flux |
| $k$ | imaginary refractive index |
| $n$ | real refractive index |
| $s$ | sideward scattering fraction |
| $S$ | arbitrary direction |
| $x$ | Cartesian coordinate. |

Greek symbols

| | |
|---|---|
| $\theta$ | particle polar angle |
| $\lambda$ | wavelength |
| $\mu$ | $\cos(\xi)$ |
| $\xi$ | slab polar angle |
| $\sigma_s$ | scattering coefficient |
| $\phi$ | particle azimuthal angle |
| $\Phi$ | mixture phase function |
| $\psi$ | slab azimuthal angle |
| $\omega$ | solid angle. |

Subscripts and superscripts

| | |
|---|---|
| i | incident |
| $x, y, z$ | Cartesian coordinate directions |
| $\hat{\lambda}$ | spectral quantity |
| $\hat{}$ | approximate. |

$$\frac{dI_x^+}{dx} = -(2a+2B\sigma_s)I_x^+ + 2B\sigma_s I_x^- \quad (2a)$$

$$\frac{dI_x^-}{dx} = (2a+2B\sigma_s)I_x^- - 2B\sigma_s I_x^+. \quad (2b)$$

This simplification has its greatest application in planar systems where the radiation transfer is mainly perpendicular to the plane and where scattering is important. (If scattering is not important the integral does not appear and other methods can also be used to obtain a solution.) The same technique can be used in two or three dimensions to yield four or six similarly coupled equations, respectively, though defining the solid angles—which are no longer hemispheres—becomes more difficult.

A feature of all flux models is the appearance of scattering fractions: $B$ (for backward scattering) in the two-flux model, and $f$, $b$ and $s$ (for forward, backward and sideward) in more dimensions. The reduction of the integral governing the scattering contribution to $i'$ in equation (1) gives rise to these factors which determine what fraction of the total light scattered from a volume element is directed into the forward, backward and sideward directions as measured with respect to the medium. In the basic scattering process, light is scattered in all directions from a differential volume in the medium with the intensity in any direction proportional to the mixture phase function $\Phi(\theta, \phi)$. The mixture phase function, which is an average of the single particle phase functions over the particle size distribution [3], gives the radiation scattered into a solid angle about $(\theta, \phi)$ divided by the light that would be scattered if the scattering were isotropic. The angle $\theta$ is measured from the direction of the incident light, and the angle $\phi$ is the corresponding azimuthal angle. We will assume here that there is no $\phi$ dependence of the scattered light which is valid for spherical particles, or for a collection of randomly oriented particles, and covers most cases. (It is not true for instance for scattering by fibers when the fibers have a preferred direction.) Thus we have a mixture phase function $\Phi(\theta)$ which will be considered as given. For an ensemble of particles it can be measured or calculated, e.g. by using Mie theory, if the particles are spherical and the size distribution is known.

This mixture phase function is used to determine the backward scattering fraction $B$ for use in the two-flux equations. There are two ways to accomplish this, one of which is to simply integrate the mixture phase function over the rearward hemisphere

$$\tilde{B} = \frac{1}{4\pi}\int_0^{2\pi}\int_{\pi/2}^{\pi}\Phi(\theta)\sin\theta\,d\theta\,d\phi \quad (3)$$

where the factor $1/4\pi$ assures the proper normalization. The backward scattering fraction determined in this way is denoted by $\tilde{B}$ but is only approximate, however. This is because the angles used to define the phase function with respect to the direction of incident radiation are not in general the same as the angles used to define a direction in the planar geometry. In the one-dimensional slab geometry the angle $\xi$ is the polar angle measured from the positive $x$-axis, and $\psi$ is the azimuthal angle. There is a one to one correspondence between $(\theta, \phi)$ and $(\xi, \psi)$ only when the incident radiation is parallel to the $x$-axis. Thus, as is further discussed by Brewster [4], for an exact treatment an integration over all incoming angles $(\xi', \psi')$ must be performed and in each instance the fraction of the scattered energy that goes forward, or respectively backward, with respect to the medium must be calculated. This yields a triple integral

$$B = \frac{1}{2\pi}\int_0^1\int_{-1}^0\int_0^{\pi}\Phi[\theta(\mu,\mu',\psi')]\,d\psi'\,d\mu'\,d\mu \quad (4)$$

where the variable $\mu = \cos(\xi)$ has been substituted. The relation between the scattering angle $(\theta)$ and the incoming $(\xi', \psi')$ and outgoing $(\xi, \psi)$ directions expressed in the spherical coordinates fixed in the medium is given by Ozisik [5] as

$$\cos(\theta) = \cos(\xi)\cos(\xi') + \sin(\xi)\sin(\xi')\cos(\psi - \psi'). \quad (5)$$

Equations (4) and (5) can be used together to calculate $B$.

For a comparison between the approximate and the exact methods, calculations were carried out for two media, one composed of purely scattering particles with an index of refraction of $1.21+0.0i$ (which matches the system studied by Brewster and Tien [6]), the other of absorbing particles with a refractive index of $1.8+0.75i$ (corresponding roughly to carbon). First, the phase function was determined for various particle size parameters $(\pi D/\lambda)$ using Mie theory [7]. Then $\tilde{B}$ and $B$ were calculated via equations (3)–(5). The results are shown in Figs. 1 and 2. It can be seen that for small size parameters, less than about 0.3, $\tilde{B} \approx B \approx 0.5$. This is because in this regime the particles are Rayleigh scatterers and the phase function is symmetric about the forward and backward directions. For larger values of the size parameter $B$ and $\tilde{B}$ both decrease, with the latter dropping to a lower value. In this region the backward scattering fraction may be underestimated by up to 9 times for the worst case if the approximate formula is used. The errors are clearly larger for the non-absorbing mixture. In fact, for absorbing particles $B$ and $\tilde{B}$ both approach the same value, in this case 0.06, if the size parameter is large enough. This is because for large, opaque, specular spheres the phase function is isotropic, except for the large forward peak due to diffraction whose contribution to $B$ decreases as the size parameter increases. For an isotropic phase function equations (3) and (4) yield the same result: $\Phi/2$.

## SIX-FLUX MODEL

The six-flux model is an extension of the two-flux model to three dimensions. By assuming constant intensity over six

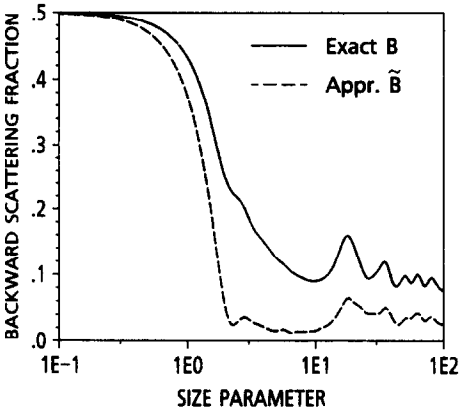


FIG. 1. Comparison of exact and approximate two-flux backward scattering fractions vs size parameter for $n = 1.21$ and $k = 0.0$.

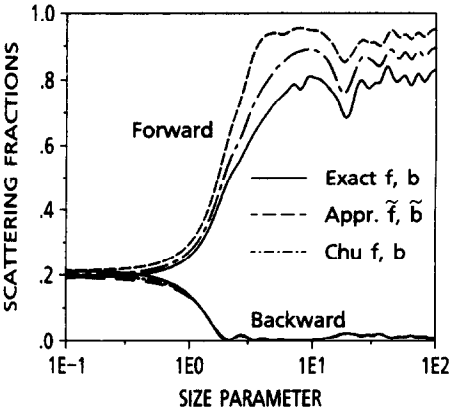


FIG. 3. Comparison of exact and approximate six-flux scattering fractions vs size parameter for $n = 1.21$ and $k = 0.0$.

solid angles centred about the axes, six coupled equations of the type [8, 9]

$$\frac{dI_x^+}{dx} = -\frac{2}{3}[a+(1-f)\sigma_s]I_x^+ + \frac{2}{3}b\sigma_s I_x^- + \frac{2}{3}s\sigma_s(I_y^+ + I_y^- + I_z^+ + I_z^-) \quad (6)$$

are obtained. In order to calculate the scattering parameters a pyramidal shaped solid angle—formed by connecting the corners of a cube to its centre—is centred around each of the six positive and negative axis directions. The incoming radiation intensity is assumed to be constant within one of the pyramidal solid angles and the radiation scattered into the six solid angles is calculated. By symmetry the four sideward scattering fractions are all the same. In principle, the integration is exactly as in the two-flux case except that the limits are complicated by the integration over squares in spherical coordinates.

In order to make the problem more tractable, several approximations are possible. First, an $\tilde{f}$ and $\tilde{b}$ can be defined which are calculated as in the two-flux case by assuming that the incoming radiation is all directed along the axis. The light scattered into the forward and backward pyramids is determined and the sideward scattering fractions are found by $s = (1-f-b)/4$ [8]. A second possibility is to account for the diffuse incident radiation by assuming it to be contained within a cone-shaped solid angle centred on the axis that subtends the same solid angle as the pyramid. This shape simplifies the integration considerably, and is also used for the scattered radiation. The appropriate formulas are

$$f = \frac{3}{4\pi}\int_{2/3}^{1}\int_{-1}^{-2/3}\int_{0}^{2\pi}\Phi(\theta)\,d\psi'\,d\mu'\,d\mu \quad (7a)$$

$$b = \frac{3}{4\pi}\int_{-1}^{-2/3}\int_{-1}^{-2/3}\int_{0}^{2\pi}\Phi(\theta)\,d\psi'\,d\mu'\,d\mu \quad (7b)$$

which are analogous to equation (4). For test cases [10] virtually no difference was found between the cone and the pyramid integration, so the former is used here due to its relative simplicity. The third possibility is to employ equations suggested by Chu and Churchill [8] which include the full hemisphere as an integration region, but weight the phase function with a $\cos^2(\theta)$ factor.

The results of these three calculations are shown in Figs. 3 and 4 for the two sample media. It can immediately be recognized that all three methods yield the same back scattering factor except for small size parameters ($<0.2$) where 5–10% differences are noted. For small particles (size parameter less than 0.5) the forward scattering is also nearly the same for each method, and indeed the same as the back scattering at about 0.2. This gives a sideward scattering fraction of 0.15, which is lower than 0.2 because small particles do not scatter isotropically, but do scatter symmetrically forwards and backwards (Rayleigh scattering). At larger size

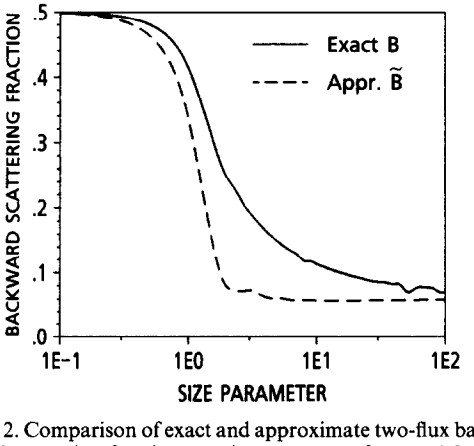


FIG. 2. Comparison of exact and approximate two-flux backward scattering fractions vs size parameter for $n = 1.8$ and $k = 0.75$.

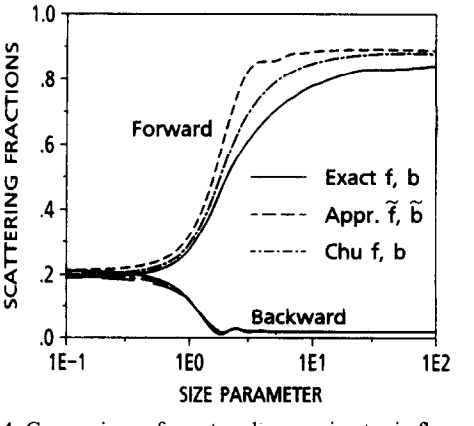


FIG. 4. Comparison of exact and approximate six-flux scattering fractions vs size parameter for $n = 1.8$ and $k = 0.75$.

parameters the forward scattering results diverge, with the first approximation (incident radiation along axis) significantly overestimating the forward scattering fraction as was also found in the two-flux case. The Chu and Churchill method also gives too high a value, but to a lesser extent. The ripples seen in the curves are the result of the high number of peaks in the phase function, the angular position of which depend strongly on the size parameter. For a cloud of particles of slightly different sizes the mixture phase function, and hence $f$ and $b$, would cease to oscillate. Again, as in the two-flux case, for absorbing particles the scattering fractions approach practically the same limit as the size parameter increases.

## SUMMARY AND CONCLUSIONS

This paper has presented exact methods of calculating the scattering fractions for use in the two- and six-flux radiation models, as well as some approximations which can simplify the integration of the mixture phase function over the appropriate solid angle. For particle size parameters less than 0.3 the scattering fractions are constants, and the values $B = 0.5$ for the two-flux model and $f = b = 0.2$, $s = 0.15$ for the six-flux model can be used. For larger size parameters, the scattering fractions must be calculated, especially in the case of a purely scattering medium. In the two-flux case, the integration method developed by Brewster should be used, unless the particles are large and absorbing in which case the simplification is allowable. For the six-flux model the method of Chu and Churchill can be employed for a rapid, if somewhat too high, estimate of $f$ and $b$, or the cone integration can be applied for a fully valid approximation. In both cases tested the Chu and Churchill method was better than the assumption of a single angle of incidence along the axis and the integration far easier than over the cone. It is therefore recommended especially in problems where many determinations of the scattering fractions are necessary. In all cases of weakly or non-absorbing particles care should be taken to average over a few particle sizes rather than take a nominal size (unless the particles really all have one diameter), since the strong variations in the phase function lead to oscillations in the calculation of the scattering fractions.

## REFERENCES

1. R. Siegel and J. Howell, *Thermal Radiation Heat Transfer*, pp. 522–544. Hemisphere, New York (1981).
2. M. Brewster, Radiative transfer in packed and fluidized beds, Ph.D. Thesis, University of California at Berkeley, California (1981).
3. F. Miller, Radiative heat transfer in a flowing gas–particle mixture, Ph.D. Thesis, University of California at Berkeley, California (1988).
4. M. Brewster, *Direct Contact Heat Exchange* (Edited by F. Kreith and R. Boehm). Hemisphere, New York (1988).
5. M. Ozisik, *Radiative Transfer and Interactions with Conduction and Convection*. Wiley, New York (1983).
6. M. Brewster and C. L. Tien, Examination of the two-flux model for radiative transfer in particular systems, *Int. J. Heat Mass Transfer* **25,** 1905–1907 (1982).
7. C. Bohren and D. Huffman, *Absorption and Scattering of Light by Small Particles*. Wiley, New York (1983).
8. C. Chu and S. Churchill, Numerical solutions of problems in multiple scattering of electromagnetic radiation, *J. Phys. Chem.* **59,** 855–863 (1955).
9. F. Miller and R. Koenigsdorff, Theoretical analysis of a high temperature small-particle solar receiver, *Proc. 5th Symp. on Solar High Temperature Technologies*. International Energy Agency, Davos (1990).
10. R. Ziegler, Auswahl, Implementierung und Test von Berechnungsverfahren zur Ermittlung der optischen Parameter von Gas-Partikelgemischen, Diplomarbeit, Deutsche Forschungsanstalt für Luft- und Raumfahrt und Institut für Thermodynamik und Wärmetechnik, Stuttgart (1989).